

Critical behavior of the optical absorption edge in CdCr₂Se₄

I. Balberg and A. Maman

The Racah Institute of Physics, The Hebrew University of Jerusalem, Jerusalem 91000 Israel

(Received 9 August 1976)

The first measurements of the temperature dependence of a semiconductor's optical gap $E_g(T)$ in the close vicinity of a critical point T_c are reported herein. The measurements were carried out on the ferromagnetic semiconductor CdCr₂Se₄ ($T_c = 130.6^\circ\text{K}$) for which a well-known red shift of $E_g(T)$ with decreasing temperature occurs. The results in the temperature range $10^{-1} \geq |t| \equiv |T/T_c - 1| \geq 5 \times 10^{-4}$ are analyzed in terms of the specific-heat universal constants: the exponents α^\pm and the ratio A^+/A^- . It is found that with the constraint $T_c^+ = T_c^-$ the values $\alpha^+ = -0.020 \pm 0.004$, $\alpha^- = -0.038 \pm 0.003$, and $A^+/A^- = 0.60 \pm 0.05$ are obtained. If the constraints $\alpha^+ = \alpha^- = -0.020$ or $\alpha^+ = \alpha^- = -0.038$ are applied the ratio $A^+/A^- = 0.64 \pm 0.05$ is found. The present results, in accord with previous results of magnetization measurements, indicate clearly that the above $|t|$ range is a transition region between mean-field and asymptotic critical behavior. This is understood to be due to the relatively long-range magnetic interactions in the present material.

I. INTRODUCTION

For the past ten years the temperature dependence of the optical-absorption edge was studied in many ferromagnetic semiconductors.^{1,2} It was found that in all materials investigated the absorption edge exhibited a red shift when the temperature T decreases.^{2,3} In the materials EuO, EuS, and CdCr₂Se₄, for which semiquantitative studies were made, it was found that this temperature dependence can be described by model spin-spin correlation functions,^{1,4,5} or by experimental quantities that are proportional to the derivatives of these functions (such as the specific heat or the coefficient of thermal expansion).^{1,6}

While both theoretical^{4,5,7,8} and experimental investigations^{1,2} of the optical gap E_g (identified by the optical-absorption edge), were concerned only with the general features of $E_g(T)$, no attention was given to the exact dependence in the close vicinity of the critical temperature T_c . Only very recently, Alexander, Helman, and Balberg,^{9,10} have considered this temperature region and have predicted the critical temperature and magnetic field dependence of E_g . Motivated by these predictions, we have carried out optical-absorption measurements on CdCr₂Se₄ crystals in a closer vicinity of the critical point than previously reported. This material was chosen because it is one of the purest and best characterized magnetic semiconductors.

As is shown in Appendix A, in the critical region the magnetic contribution to the optical band gap $\Delta E = E_g - E_c$, where $E_c = E_g(T = T_c)$ can be given in the case of a fixed valence band by

$$\Delta E = \left(\frac{1}{2}JS\right) \left\{ -|t|^\beta + [J(S+1)/4E_k](\kappa_0/\Lambda)^{1+\eta} \times (\kappa_0/k)^{(1-\alpha^-)/\nu-1-\eta} U^- \right\} \quad (1)$$

for $T < T_c$, and without the first term but with α^+ and U^+ instead of α^- and U^- for $T > T_c$. Here $t = (T - T_c)/T_c$, β , α^\pm , ν , and η are the usual exponents,^{11,12} J is the exchange coupling constant between the conduction electron in the state \vec{k} and the localized spin \vec{S} of the magnetic ion, $E_k = \hbar^2 k^2 / 2m^*$ where m^* is the electron effective mass, $k = |\vec{k}|$ and $(\kappa_0)^{-1}$ is the magnetic ions interaction range. U^\pm are terms proportional to the magnetic energy the form of which can be given by

$$U^+ = (A^+/\alpha^+) [t^{1-\alpha^+}/(1-\alpha^+) - t] + B^+ t \quad (2)$$

for $T > T_c$, and

$$U^- = -\{(A^-/\alpha^-)[|t|^{1-\alpha^-}/(1-\alpha^-) - |t|] + B^-|t|\} \quad (3)$$

for $T < T_c$. Here A^\pm and B^\pm are constants that are expected to be proportional to the corresponding constants of the specific heat.¹³⁻¹⁵ Since the coefficients of U^+ in Eq. (1) are not exactly known we shall incorporate them into A^+ and B^+ and thus these quantities will have the dimensions of energy. It should be pointed out that Eq. (1) represents the shift of the bottom of the conduction band rather than the optical gap which depends also on the temperature behavior of the valence band. The true optical gap depends on the difference between the two dependences.

In the mean-field region, where the Landau theory applies, i.e., for $|t| > t_G$, t_G being the Ginzburg reduced temperature,^{9,11} the theoretical results can be more conveniently represented by the derivatives¹⁰

$$\frac{dE_k}{dT} \propto -|t|^{-1/2} \quad (4)$$

for $T < T_c$, and

$$\frac{dE_g}{dT} \propto \left(\frac{1}{k} - \frac{\pi^2}{2\Lambda} \right) \kappa_0 t^{-1/2} \quad (5)$$

for $T > T_c$ and $k > \kappa_0 t^{1/2}$, since in the mean-field region $\beta = \nu = \frac{1}{2}$. The first term in Eq. (5) originates from the contribution of the long-range fluctuations and coincides with the molecular field results of Hass,⁸ while the second term originates from the normalization of the Ornstein-Zernike function⁹ and accounts for the short-range fluctuations. It is apparent that as long as $5k < \Lambda$, where Λ is the effective radius of the Brillouin zone, the first term will dominate.

According to this theory one would expect a transition from the behavior of Eq. (1) to the behavior of Eqs. (4) and (5) around t_G . The typical value of t_G for magnetic transitions¹¹ is of the order of 10^{-2} .

The measurements described below were made in order to determine the critical behavior of $E_g(T)$. Since this has not been done before and since a specific-heat-like behavior of $dE_g(T)/dT$ is expected, any differences between the optical and specific-heat measurements should be noted. The samples needed for the optical measurements, described in Sec. II, are much smaller than those needed for specific heat and thus better homogeneity¹⁵ of the samples is provided here. On the other hand, for $T < T_c$ the present measurements may be affected by optical diffraction of magnetic domains.¹⁶ The optical measurements yield a quantity that is proportional to U^\ddagger while the specific-heat measurements determine directly dU^\ddagger/dT . The latter has "sharper" features which facilitate the computational procedure and shorten the computer iteration process. As we shall see, calculating first the derivative of $E_g(T)$ and then using a specific-heat analysis procedure introduces a systematic erroneous decrease in the α^\ddagger values obtained.

The data presented in Sec. III will be analyzed in detail, because of the novelty of the present data and because there is still no acceptable procedure of analyzing specific-heat-like data.¹³⁻¹⁵ We have chosen to follow the most recent procedure¹⁵ since it takes advantage of modern developments in computer programming and since it is quite systematic. However, in the analysis, described in Sec. IV, we have used as few constraints and as few corrections as possible. In Sec. V, the results are discussed and two conclusions are reached: (a) in the close vicinity of T_c there is no evidence for the magnetization term $|t|^\beta$; (b) the results represent a transition from mean-field magnetic energy behavior to asymptotic critical behavior of this quantity.

II. EXPERIMENTAL

The relative high purity of available CdCr_2Se_4 is quite important because in measurements of critical behavior one would like to minimize the temperature region in which "rounding"^{14,15} of the critical behavior takes place. This rounding, or the spread of T_c , in the real material depends on its homogeneity.¹⁷ Since the homogeneity is hard to directly characterize and improve, the indirect approach of improved purity and small samples can ensure a relatively high homogeneity.¹⁷ In the present study using the highest purity CdCr_2Se_4 crystals available were thinned down to 100- μm -thick samples. The crystals were grown by H. L. Pinch.¹⁸⁻²¹

The samples were well-formed hexagonal $\{111\}$ platelets with an area of 5 mm². They were prepared for the optical absorption measurements by conventional grinding and polishing techniques. The total impurities in the crystals were found by emission spectrographic analysis to be less than 500 ppm, and the crystals "grew with almost no Se deficiencies."²¹ This is apparent from the saturation moment of $5.93\mu_B$ per molecule that we found from magnetization measurements, which indicates²⁰ a stoichiometry of better than 1%. Details of the magnetization measurements on undoped, indium-doped, and silver-doped crystals will be reported elsewhere. In CdCr_2Se_4 it is known²² that 1% imperfections cause about 1 °K shift of T_c . Thus t is certainly well defined for $|t| > 8 \times 10^{-3}$. However, this estimate is quite exaggerated and a more realistic model of a Gaussian distribution of imperfections throughout the crystal volume²³ yields a lower limit of about 10^{-3} . The present measurements and resistivity measurements²⁴ on many In and Ag doped CdCr_2Se_4 crystals indicate that for $|t| \geq 5 \times 10^{-4}$ no "rounding" of T_c was observed for 1% imperfections. Thus, the measurements were carried out for these values of t .

In the experiment, chopped light was passed through a Spex 1700 monochromator with a resolution of better than 1 Å, and wavelength reading accuracy of 0.1 Å. The monochromatic light was split, and the ratio between the signal of the light transmitted through the sample and the signal of a reference light beam was monitored. This was done by using two identical silicon photodiodes, two lock-in amplifiers and an electronic divider. The sample was mounted in a Dewar with a cold finger specially designed to give maximum thermal sensitivity and stability when coupled to an Artronix temperature controller. Both the temperature sensitivity and stability, monitored by two P_t thermometers calibrated to an accuracy of

3×10^{-5} °K, were better than 5 mK. With the calibration and the digital reading of the thermometers resistances, the absolute temperature was determined to an accuracy of 10^{-2} °K. In the measurement, the ratio of the two signals represents practically the changes in the absorption coefficient since the changes in the reflectivity²⁵ over the interesting temperature region can be neglected. This was confirmed over the temperature range $134 \geq T \geq 127$ °K for which the critical behavior was studied. For a fixed photon energy in the range $1.3 \geq h\nu \geq 1.2$ eV the ratio has changed by about a factor of 2 upon raising the temperature from 127 to 134 °K. On the other hand the reflectivity has then changed only by 1%. The last result is also in accord with previous measurements of the reflectivity.²⁵ Thus, we did not correct for the reflectivity in these measurements and the measurements were carried out by fixing the ratio of signals and then finding for each temperature the wavelength corresponding to the selected ratio. With the present system and crystals we had a sensitivity of $60 \text{ \AA}/^\circ\text{K}$ in the vicinity of T_c and thus changes of wavelength due to variations of 50 mK were easily and accurately monitored.

III. EXPERIMENTAL RESULTS

In order to use the experimental procedure described above we had first to determine the photon energy dependence of the absorption coefficient $K(h\nu)$. Previously, only calculated²⁵ or qualitative²⁶ accounts of this dependence were reported. In addition to the single crystals, the measurements were carried out also on a single-crystal film¹⁹ to help in the determination of the absorption edge. The results, shown in Fig. 1, were obtained by computing K from the measured optical density, after correction for the reflectivity was made.^{25,27} The dashed line shown in Fig. 1 is believed to represent the absorption edge of CdCr_2Se_4 while the deviations from this line at lower photon energies originate apparently from absorption due to various imperfections.²⁶ The shape of the absorption edge, namely, $dK/d(h\nu)$, was found here, as well as in the early work of Harbeke and Pinch,¹⁹ to be independent of temperature in the temperature range $300 \geq T \geq 80$ °K. In practice, the effect of temperature is to cause the "dashed line" to shift parallel to itself in this temperature region. For the present work we had to define an "absorption edge" by a K that will be low enough to be consistent with the assumptions made in the theory,^{9,10} and that will be high enough to avoid the influence of the absorption due to imperfections. It can be seen from Fig. 1 that $K = 200 \text{ cm}^{-1}$ is the best choice, and thus it was

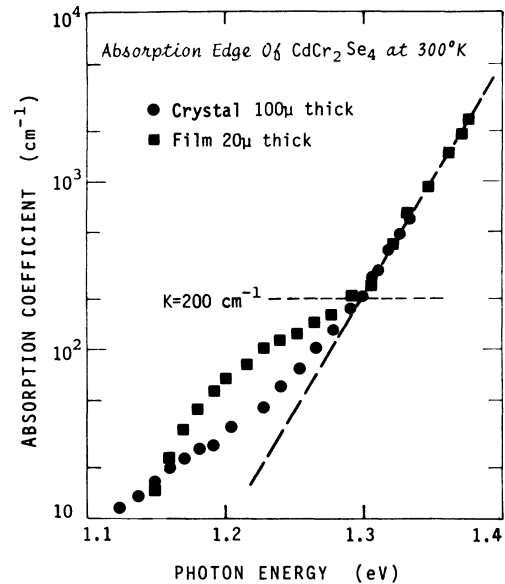


FIG. 1. Photon-energy dependence of the absorption coefficient of CdCr_2Se_4 in the vicinity of the absorption edge.

used throughout this work to define the absorption edge.

Once K was chosen the $E_g(T)$ measurements were carried out, as described in Sec. II, between 100 and 300 °K. The results obtained on the crystal, the absorption edge of which is shown in Fig. 1, are presented in Fig. 2. The general features of

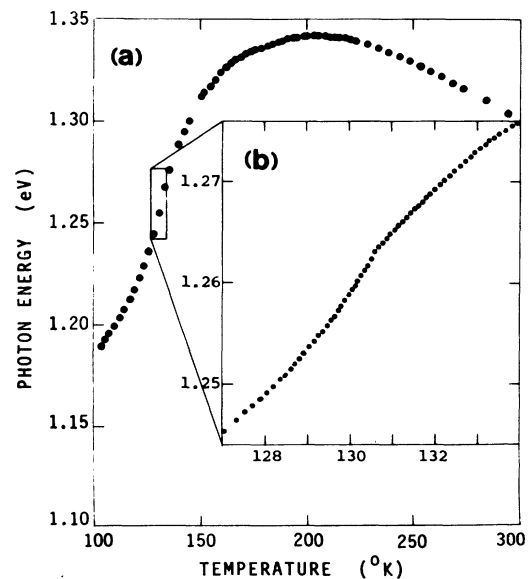


FIG. 2. Temperature dependence of the optical "absorption edge" of CdCr_2Se_4 (a) and the details of this dependence in the vicinity of T_c , (b). The "absorption edge" is defined by $K = 200 \text{ cm}^{-1}$.

the data in Fig. 2(a) are well known from the early work of Harbeke and Pinch.¹⁸ However, the changes of $E_g(T)$ observed here in the temperature range 130 ± 30 °K are 20% larger than the corresponding ones reported in the early work. This is attributed to the relatively high purity of the present crystals, since it was found both in EuO,²⁸ and CdCr₂Se₄,²⁹ that impurities cause a decrease of the total red shift of the absorption edge. As illustrated by Fig. 2(a) the absorption edge has an inflection point around 130 °K. The vicinity of this point is shown in more detail in Fig. 2(b). In view of this detailed datum, one can appreciate the magnitude of the red shift since in the same temperature range the "blue" shift of conventional semiconductors is about one or two orders of magnitude smaller.

From the predictions given above by Eqs. (1), (4), and (5) a divergence ($\alpha^+ > 0$) or a cusp ($\alpha^+ < 0$) are expected to be observed in dE_g/dT at the vicinity of T_c . We have thus computed the temperature derivative of $E_g(T)$ in the vicinity of the above inflection point, using the detailed data of Fig. 2(b). The derivative was calculated by the method of sliding averages³⁰ with five-point sets. The results are found to display a specific-heat-like peak with a maximum at 130.55 °K. This is shown in Fig. 3. Since the measurements in the vicinity of this temperature were taken at 130.45, 130.55, and 130.62 °K the present procedure allows

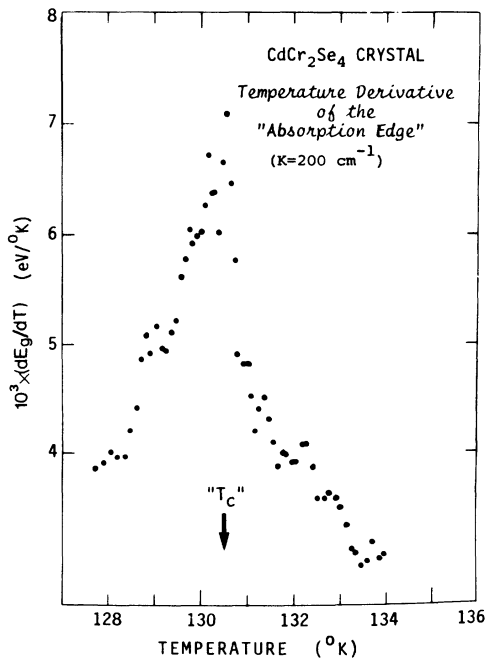


FIG. 3. Temperature dependence of the temperature derivative of the optical "absorption edge" in CdCr₂Se₄.

the identification of the point of maximum derivative T_c as being between 130.45 and 130.62 °K. A selection of T_c outside this range by other criteria²³ will not be in accord with Eqs. (1)–(5) when approaching T_c from both above and below. The derivative exhibits quite a sharp peak and there is no indication of apparent "rounding" of this peak (see below). However, in order to assign significant values to α^+ , β , A^+/A^- , and T_c , the results shown in Fig. 3 can not be used. This can be seen in the sliding averages method where a parabola is fitted to a set of adjacent points, and the computed derivative of the set middle point is considered the "true" derivative. The sliding is done by making each point a middle point of a set. When the number of points in the set m is large, the "scatter" of the points is small, but the peak in the vicinity of T_c is "smeared" and vice versa. In our case, for example, dE_g/dT at 130.55 °K was reduced by 20% when m was increased from $m = 2$ to $m = 9$. Since the use of derivatives is quite common in analysis of critical resistivity measurements, we shall demonstrate the disadvantages of the differentiation in the next section. To avoid these difficulties, we have analyzed the present data by fitting a function of the type given in Eqs. (1)–(3) to the results of the measurements.

IV. ANALYSIS OF RESULTS

In the analysis we have carried out a nonlinear four- (or five-) parameter least-squares fit to determine the constants of Eqs. (2), (3), their standard errors and their uncertainties. The latter will be given here by the limits of confidence of each parameter. These computations were done using Marquardt maximum-neighborhood method³¹ that was adopted previously for the analysis of specific-heat data.^{15, 32} This method is based on finding the function of the best fit F of the parameters p_i that yield the minimum of the function R defined by

$$R(p_1, p_2, \dots, p_i) = \sum_{i=1}^N [F(p_1, p_2, \dots, p_i, T_i) - E_g(T_i)]^2, \quad (6)$$

where $E_g(T_i)$ are the experimental points and N is their number. In the iterations the "flow" of the parameters is in the direction where $\text{grad}R$ obtains its largest value. In principle, R may have more than one local minimum and thus in order to find the "deepest" as well as a "reasonable" minimum, the best possible initial values of the parameters should be provided. This is especially true when the temperature dependence of the data has a relatively weak temperature dependence [for example,

in the present case the temperature dependence of $E_g(T)$ is weaker than that of dE_g/dT . Here, in view of the results given in Sec. III, values of $T_c = 130.55$ K and $E_c^{\pm} = 1.26$ eV were used in the initiation of the iteration process.

Since the analysis of specific-heat-like data^{32,33} is "perhaps the most difficult critical data to categorize and understand"¹¹ one usually makes some assumptions or imposes some constraints^{14,32} in order to determine the critical behavior from the data. In this work we have tried to minimize these, especially since in variance with specific-heat data¹⁵ (due to the *a priori* possibility of a magnetization term for $T < T_c$) the use of the relations between the parameters below and above T_c is more dubious.

In the present analysis we assume that the data has to be described by the functions F^{\pm} that are given by

$$F^{\pm} = -M^{\pm} |t|^{\beta} + U^{\pm} + E_c^{\pm}, \quad (7)$$

where $M^{\pm} = 0$ [see Eqs. (1)–(3)]. The second assumption is that the "best" fit of the parameters, as determined by the computational procedure mentioned, does indeed provide the "true" parameters.

It is clear that the more data points involved, the more reliable is the analysis, and we shall try to interpret the results using all the data points. A unique set of parameters is of course questionable over the entire temperature range since a transition from mean-field behavior to asymptotic behavior is expected¹¹ around $|t| \approx 10^{-2}$. This as well as other assumptions that were made will be discussed below. We shall list all the parameters obtained in the cases which we consider significant. The limits of confidence of the parameters will be given explicitly for T_c^{\pm} , α^{\pm} , and E_c^{\pm} , while for the ratio A^+/A^- the uncertainty will be determined by the relative uncertainties obtained for A^+ and A^- .

The first problem of the present work is to find the role of the magnetization term $M^{\pm} |t|^{\beta}$, since this is the only predicted difference between the critical behavior of the optical absorption edge and that of the magnetic energy. To do this let us assume that $T_c = 130.55$ K and that there is a unique set of parameters that describes the critical behavior over the entire temperature range under study, i.e., $10^{-1} \geq |t| \geq 5 \times 10^{-4}$. Then, using F^- [Eq. (7)] with the various β 's: $\beta = 0.5, 0.45$ (the value obtained from magnetization measurements³⁴), $0.4, 0.33$, and $\beta = 0$, for $T < T_c$ and F^+ for $T > T_c$, we have obtained the following results: While $0.024 \leq \alpha^+ = 0.023 \leq 0.026$, α^- has changed gradually from $-0.074 \leq \alpha^- = -0.071 \leq -0.068$, for $\beta = 0$ to $-0.154 \leq \alpha^- = -0.147 \leq -0.141$, for

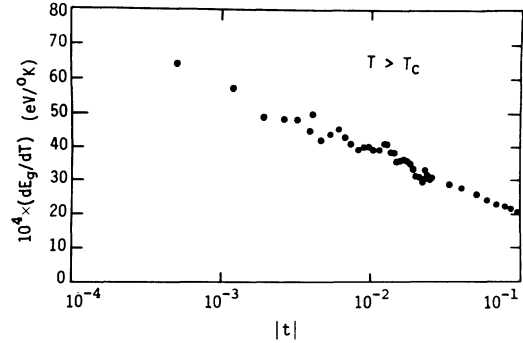


FIG. 4. Semilog plot of the temperature derivative of the optical "absorption edge" for $T > T_c$. $T_c = 130.55$ K is defined by the position of the peak in Fig. 3.

$\beta = 0.5$. Correspondingly A^+/A^- has decreased from 0.63 ± 0.06 to 0.41 ± 0.04 . The value of M^- was two orders of magnitude smaller than A^+ and was found to decrease by another order of magnitude with decreasing β . The standard errors of all parameters have doubled with β increasing from $\beta = 0$ to $\beta = 0.5$. In view of the theoretical predictions^{12,35} $\alpha^+ = \alpha^-$, $A^+ \approx A^-$ and the increasing error we can conclude that improvement will be achieved if the magnetization term is omitted. Thus we shall keep the constraint $M^- = 0$ in the analysis to follow.

For illustration of the above discussion let us present the results of dE_g/dT , shown in Fig. 3, on a semilog scale. This is done for $T > T_c$ in Fig. 4 and for $T < T_c$ in Fig. 5. It is seen that for $|t| \geq 2 \times 10^{-3}$ a logarithmic behavior is observed while for lower $|t|$ values a "sublogarithmic" ($-\alpha^- > 0$) behavior is observed. If we would have added here a term $M^- |t|^{\beta-1}$ that has a "superlogarithmic" ($\beta - 1 < 0$) behavior, then in order to account for the data, α^- should have been more negative than in the case of $M^- = 0$, thus increasing its deviation from α^+ . The role of a negative correction term^{15,31} Dt^x , where $1 > x > 0$, will also be

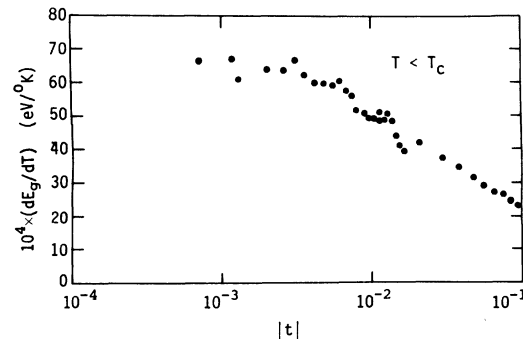


FIG. 5. Semilog plot of the temperature derivative of the optical "absorption edge" for $T < T_c$. $T_c = 130.55$ K.

to lower the fitted function in the large $|t|$ end, and thus to increase the curvature of the fitted function. This increase is expressed by a lower¹⁵ value of α^\pm . In view of the above results we have chosen to proceed without introducing correction terms.

So far we have assumed $T_c = 130.55$ °K as obtained from the derivative. The role of a T_c change is also apparent from Figs. 4 and 5. If we let T_c be higher than 130.55 °K (but smaller than 130.62 °K) α^+ will decrease and α^- will increase compared with values obtained with 130.55 °K. On the other hand, if we take $130.55 > T_c \geq 130.45$ °K, α^+ will increase and α^- will decrease compared with the $T_c = 130.55$ °K values. Hence the most reliable parameters of the functions F^\pm , to be fitted, will be obtained by using T_c as a parameter that has to be enclosed in the "experimental" interval of $130.62 \geq T_c \geq 130.45$ °K. The fit of F^+ to the data points shown in Fig. 2(b) has yielded the following results. For the $T > 130.55$ °K data points we found the parameters

$$\begin{aligned} 130.59 \leq T_c^* &= 130.619 \leq 130.65 \text{ °K}, \\ 126.27 \leq E_c^* &= 1.2628 \leq 1.2629 \text{ eV}, \\ 0.1112 \leq A^* &= 0.1119 \leq 0.1125 \text{ eV}, \\ 0.00604 \leq B^* &= 0.0082 \leq 0.0103 \text{ eV}, \end{aligned} \quad (8)$$

and

$$-0.024 \leq \alpha^* = -0.020 \leq -0.018.$$

For the $T < 130.55$ °K data points if we let T_c^- be a parameter we get $130.51 \leq T_c^- = 130.55 \leq 130.58$ °K, $-0.074 \leq \alpha^- = -0.069 \leq -0.066$, and $0.202 \leq A^- = 0.203 \leq 0.204$ eV. On the other hand we know¹⁵ that the results are meaningful only if $T_c^+ = T_c^-$ and thus we have applied this constraint.¹⁵ However, in view of the doubts concerning the data below 130.55 °K (possible magnetization term and domain effects) we have chosen $T_c^- = T_c^+ = 130.619$ °K. With this T_c we get

$$\begin{aligned} 1.2630 \leq E_c^- &= 1.2632 \leq 1.2633 \text{ eV}, \\ 0.1844 \leq A^- &= 0.1855 \leq 0.1867 \text{ eV}, \\ -0.1157 \leq B^- &= -0.1117 \leq -0.1077 \text{ eV}, \end{aligned} \quad (9)$$

and

$$-0.041 \leq \alpha^- = -0.038 \leq -0.035.$$

These results justify, *a posteriori* the constraint, since the values obtained now are in better agreement with the expectations^{12,14} $\alpha^+ = \alpha^-$ and $A^+/A^- \approx 1$. If we try the other constraint¹⁵ $\alpha^+ = \alpha^-$ and choose for the above reason $\alpha^- = \alpha^+ = -0.020$ we get

$$\begin{aligned} 1.2631 \leq E_c^- &= 1.2632 \leq 1.2633 \text{ eV}, \\ 0.1748 \leq A^- &= 0.1739 \leq 0.1730, \\ -0.0951 \leq B^- &= -0.0918 \leq -0.0884. \end{aligned} \quad (10)$$

Comparison of the results of Eqs. (9) with those of Eqs. (10) shows that A^+/A^- is "improved" in the latter case yielding 0.64 ± 0.05 rather than 0.60 ± 0.05 for the first case. Further, the standard error is reduced by a factor of 10 for A^- , a factor of 5 for B^- , and a factor of 2 for E_c^- , when the constraint is made. For completeness it should be pointed out that the ratio $A^+/A^- = 0.64 \pm 0.05$ is also obtained if the constraint $\alpha^+ = \alpha^- = -0.038$ is imposed. This case has yielded $A^+ = 0.1190 \pm 0.0006$, $B^+ = -0.003 \pm 0.002$, $E_c^+ = 1.2628 \pm 0.0001$ and somewhat smaller standard errors compared with those of the parameters given in Eq. (8).

Another possible constraint is to impose the continuity¹⁵ of the functions F^+ and F^- as well as their derivatives (for the $\alpha^\pm < 0$ case) at T_c . These conditions are

$$E_c^+ = E_c^- \quad (11)$$

and

$$-(A^+/\alpha^+) + B^+ = -(A^-/\alpha^-) + B^-. \quad (12)$$

While the first condition is well satisfied above [see Eqs. (8)–(10)], the second condition [Eq. (12)] is in better agreement with the unconstrained results [Eqs. (8) and (9)]. This agreement is good enough to reverse the argument, i.e., imposing the continuity of the derivative yields the results of Eqs. (9). As we shall see in Sec. V the differences between the two sets of results [Eqs. (9) and (10)] are not significant in the framework of the present interpretation.

We should note that in all computations a larger weight is given to the closest points to the selected T_c in view of the increase of dE_g/dT as T_c is approached. We found that carrying the above procedure but eliminating the two closest points, or by dividing the right-hand side of Eq. (6) by the outweighing factor $1 + [F'(T_i)]^2$ have not yielded results that differ significantly from those given in Eqs. (8) and (9).

To demonstrate the quality of the fits of F^+ and F^- , obtained in the analysis, with the experimental data, we show in Figs. 6 and 7, computer generated plots of these functions, as well as the corresponding experimental points. For Fig. 6 the parameters of Eq. (8) were used while for Fig. 7 those of Eq. (9) were used. As can be seen, the present fits are as good as those obtained for specific-heat data^{15,32} (see, for example, Fig. 3 in Ref. 15).

Following the analysis of specific-heat data^{15,32}

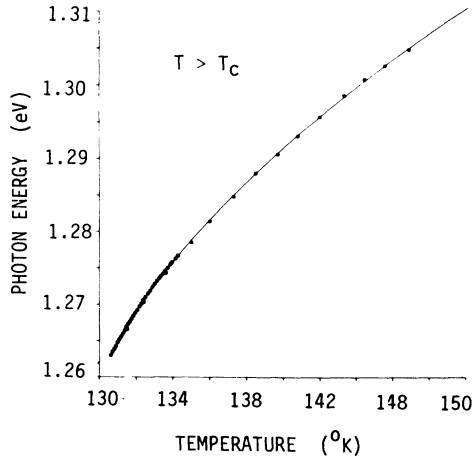


FIG. 6. Computer generated plot of the best fit to the measured $E_g(T)$ points for $T > T_c$. The parameters of the fit are given in Eq. (8).

we have also considered the effect of the $|t|$ interval on the exponents obtained. When t_{\max} is the upper limit of the interval and t_{\min} is the lower limit, we found, as in specific-heat data analysis, that α^+ and α^- decrease with decreasing $|t_{\max}|$ and $|t_{\min}|$. In our case the α^+ value, for $5 \times 10^{-3} > |t| > 5 \times 10^{-4}$, was found to be $\alpha^+ = -0.1 \pm 0.1$. The large error is expected from the smaller number of data points in this interval. For comparison we have carried out resistivity measurements²⁴ on *p*-type and *n*-type CdCr_2Se_4 . In the first case we have obtained the same results, while in the latter, where more data points were available, we got for the interval $10^{-3} \geq |t| \geq 3 \times 10^{-4}$ the values $\alpha^+ = -0.026 \pm 0.003$ and $\alpha^- = -0.068 \pm 0.008$. These results are quite in ac-

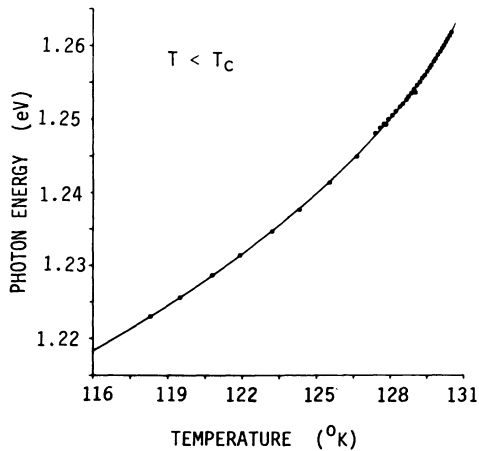


FIG. 7. Computer generated plot of the best fit to the measured $E_g(T)$ points for $T < T_c$. The parameters of the fit are given in Eq. (9). (Note the difference in scale in comparison with that of Fig. 6.)

cord with the optical data parameters given above. In this context we should point out that as long as the exponents are more positive than the theoretical predictions one can still believe that no rounding has occurred for $|t| \geq |t_{\min}|$, and that the entire t interval is not all in the scaling region where asymptotic behavior is expected to take place¹⁰ (see Sec. V). On the other hand, it is interesting to see what other behavior is consistent with the data, especially for the higher $|t|$'s where mean-field behavior is expected to be observed. For example, let us examine the interval $10^{-1} \geq |t| \geq 5 \times 10^{-2}$. In this interval, in addition to the fit demonstrated in Figs. 6 and 7, we can find a pure power law behavior of the type $|t|^\lambda$ with $\lambda^+ = 0.61 \pm 0.04$ and $\lambda^- = 0.49 \pm 0.06$. These λ^\pm values are independent of the choice of T_c within the "experimental" limits but they decrease with decreasing $|t|$ beyond 5×10^{-2} . This behavior is quite in accord with expectations from Eqs. (4) and (5). Moreover, this agreement seems to become more meaningful when the results are compared with the magnetization measurements results³⁴ that yield $\nu = \lambda^+ = 0.63$, and $\beta = \lambda^- = 0.45$. While these λ^\pm values do not necessarily indicate that we have a transition from the behavior of Eqs. (4) and (5) to that of Eq. (1) with decreasing $|t|$, they are compatible with such a transition.

In Sec. III we have pointed out that the use of the derivative is less reliable than that of the measured data. To demonstrate the remarks made there let us examine the results obtained by analyzing dE_g/dT instead of the original $E_g(T)$ data. The best fit to the data shown in Fig. 3 yields for $10^{-1} \geq |t| \geq 5 \times 10^{-4}$, the parameters $130.50 \leq T_c = 130.168 \leq 130.81$ °K, $-0.14 \geq \alpha^+ = -0.15 \geq -0.16$, $-0.04 \geq \alpha^- = -0.06 \geq -0.18$, and $A^+/A^- = 0.50$

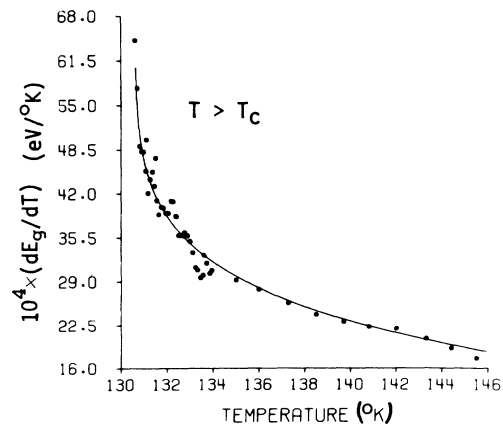


FIG. 8. Computer generated plot of the best fit to the results shown in Fig. 3 for $T > T_c$. This best fit yields $T_c = 130.618$ °K.

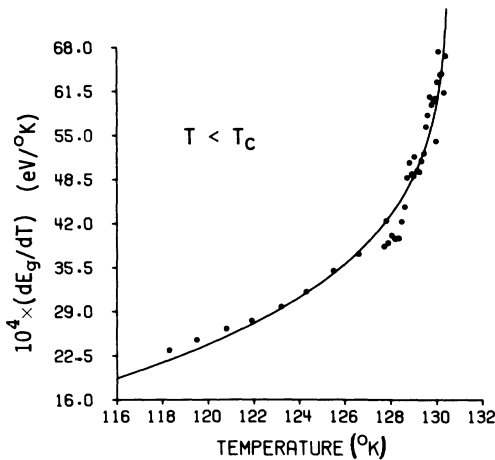


FIG. 9. Computer generated plot of the best fit to the results shown in Fig. 3, for $T < T_c$. $T_c = 130.618^\circ\text{K}$.

± 0.05 . These values are indeed smaller than the α^* values obtained from the $E_g(T)$ data, and indicate that the derivative “smears” the peak. Even with this smearing we still have quite a “scatter” of the points around the best fitted curves as is shown in Figs. 8 and 9 by the computer generated plots and the dE_g/dT computed points of Fig. 3. This relatively large scattering is especially apparent if comparison is made with Figs. 6 and 7. The above is very relevant to the analysis of the derivative of the electrical resistivity that is obtained after the differentiation of the measured data.³⁰ The alternatives are either to analyze the original data²⁴ or to measure directly the derivative by using an ac measurement technique.³⁵

V. DISCUSSION

The first point that should be examined in the present data is that there is no difference in comparison with specific-heat or resistivity data, i.e., that there is no evidence for the magnetizationlike contribution to the critical red shift for $T < T_c$. While the simple mean-field theories consider this contribution⁷⁻¹⁰ there is no evidence from all other optical-absorption data,^{1,18} which were not concerned with critical behavior, for a contribution of the magnetization term. The observation³⁶ that the conductivity activation energy in EuO, in the region $10^{-1} \geq |t| \geq 10^{-2}$, behaves as $|t|^\beta$ is of the same nature as that of the $|t|^{\lambda^*}$ behavior described in Sec. IV. Our studies in the close vicinity of T_c are thus compatible with the previous “noncritical” studies.^{1,18} If one tries to interpret the results in the region $|t| \geq 10^{-2}$ in terms of the magnetizationlike contribution, one may reach two

unreasonable conclusions: (a) in the ranges $10^{-2} \geq |t|$ and $|t| \geq 10^{-1}$ the magnetization term is unimportant and only between these $|t|$'s it is dominant, and (b) this is a unique behavior that is not in agreement with previous observations on other materials.¹ Following this we have chosen to believe that the magnetization term does not contribute to the observed $E_g(T)$ dependence in the entire $|t|$ range under study.

This conclusion is not in accord with the available theories⁷⁻¹⁰ that are based on second-order perturbation theory. However, we should recall that the theories predict the shift of the bottom of the conduction band rather than the optical gap which depends also on the position of the valence band. According to the single free-electron and mean-field theories,^{7,10} the coefficients of the magnetization and magnetic energy terms are of the same order. In the scaling region, as is shown in Appendix A, the ratio of these coefficients depends on the amplitude of \vec{k} at which the optical transition will occur. Hence $|\vec{k}|$ will determine at which $|t| = t_t$ a transition from magnetic energylike to magnetizationlike behavior will occur with decreasing $|t|$. For reasonable parameters we get (see Appendix A) $t_t \approx 10^{-2}$. For the transition, to magnetizationlike behavior, to take place beyond the studied $|t|$ interval, e.g., $|t| \leq 10^{-4}$, unreasonable large band widths have to be assumed. If only the shifts of the bottom of the conduction band and the top of the valence band are considered, it is not clear why there is no agreement between the simple theories⁷⁻¹⁰ and the experimental results concerning the nonobservation of a magnetizationlike contribution for $T < T_c$. This has led Callen⁴ to suggest a different mechanism for the red shift that is proportional to the magnetic energy. His effect was later shown to be too small to account for the data,³⁷ but in principle other energylike mechanisms^{5,38} can explain the observed behavior. On the other hand, there is evidence³⁹ in CdCr_2Se_4 for a splitting of the bottom of the conduction band [$4s(\text{Cr}^{+3})$] and the top of the valence band [$4p(\text{Se}^{-2})$] when the temperature is decreased through T_c . The fact that the magnetizationlike contribution is never observed is thus indicating that either the present theories are not adequate⁸ around $\vec{k} = 0$, or that more details of the band structure should be considered. A possibility that can account for both, the observation and the simple theories^{7,8} is that the splitting of the conduction and valence band³⁹ are such that the net change of the optical gap is dominated by the magnetic energy term. This interesting problem has not been discussed thus far in the literature, but for our present purpose it will be enough to consider that our data as well

as all other data indicate that the observed red shift is proportional to the magnetic energy.

To understand the critical behavior as characterized by the parameters found for the functions U^+ and U^- , let us first examine the theoretically^{40, 41} predicted exponents from series or ϵ expansion to order ϵ^3 (where $4 - \epsilon$ is the dimensionality of the system) for ferromagnets with two ($n = 2$) or three ($n = 3$) components of the order parameter. These as well as the exponents determined from the magnetization measurements of Miyatani³⁴ on CdCr_2Se_4 , are listed in Table I. From these experimental values and the scaling relations,⁴² that contain only the experimental exponents β , γ , and δ , we obtain some "expected" α^\pm values. These are the only available experimentally based estimates of α^\pm for the present material, since no specific-heat measurements were reported for it. It should be pointed out that there are only very few materials for which the analysis of specific-heat data is good enough^{14, 15} to yield reliable values for α^\pm . It can be seen that the above estimates are not self-consistent and are in variance with the theoretical value of -0.14 expected for the present Heisenberg ($n = 3$) ferromagnet.⁴³ This may signal the fact that the t interval studied in the magnetization measurement is not a scaling region. All the magnetization-based values of α^\pm are however larger than our findings of $\alpha^+ = -0.020 \pm 0.02$ and $\alpha^- = -0.038 \pm 0.03$. This may be considered, in view of Sec. IV, to be due to some "smearing" of T_c in the material that was used in the magnetization measurements, or to be due to the analysis of the corresponding data. In any case, the values obtained in the last column of Table I should be considered as lower limits of the real exponents.

It is now apparent that the use of the derivative or correction terms could have led to smaller α^\pm

which would have been considered erroneously to be in better agreement with the theoretical values of the Heisenberg ferromagnet. Thus, it is not enough to justify correction terms just because the iteration process converges and yields values that are closer to the theoretical predictions.¹⁵ One should at least show that the standard errors of the parameters are smaller, or that the minimum of R [Eq. (6)] is lower when correction terms are introduced.

Examination of Table I shows that the magnetically obtained exponents, i.e., β , γ , and δ (in almost the same $|t|$ interval as ours), as well as our α^\pm are between the predictions of mean field and the predictions of series or ϵ expansions for an Heisenberg ferromagnet. On the other hand, our α^\pm values that were obtained for the range $10^{-1} \geq |t| \geq 5 \times 10^{-4}$ can be representing the "real" values over this range or some averaged value between the mean-field exponents (say $\alpha^\pm \approx 0.0$ at the large- $|t|$ end) and exponents that are smaller than those obtained (say $\alpha^\pm \approx -0.1$ at the small- $|t|$ end). The latter possibility resembles the case of EuO where the "established"^{14, 15} value of $\alpha^\pm = -0.04$ may be interpreted¹⁴ as a gradual decrease of α^\pm from -0.026 to -0.09 with decreasing $|t|$. Whether the present results signal unique α^\pm values or a gradual change of α^\pm , the values obtained, and the exponents of the magnetization data,³⁴ indicate that the region under study is a transition region from mean-field to scaling behavior.

The conclusion reached above is supported by another universal quantity^{12, 14} i.e., A^+/A^- . Its value can be written¹²

$$A^+/A^- = 2^{\alpha^\pm}(1 + \epsilon)(\frac{1}{4}n) + O(\epsilon^2). \quad (13)$$

For CdCr_2Se_4 we should have $\epsilon = 1, n = 3$ in the

TABLE I. Theoretical and experimental values of critical exponents.

Exponent	Mean-field	$n = 2$ and $\epsilon = 1$		$n = 3$ and $\epsilon = 1$		Experiment ^b
		ϵ^3 ^a	Series ^a	ϵ^3 ^a	Series ^a	
β	0.5	0.351	0.348	0.367	0.373	0.447
γ	1	1.32	1.318	1.380	1.405	1.27
δ	3	4.76	4.77	4.753	4.9	4.1
α^\pm	0 ^c	-0.027	-0.02	-0.125	-0.14	-0.164 ^d -0.280 ^e -0.089 ^f

^aReferences 40 and 41.

^bResults from magnetization measurements on CdCr_2Se_4 (Ref. 34).

^cLogarithmic divergence.

^dUsing the data of Ref. 34 with the scaling relation $\alpha = 2 - 2\beta - \gamma$.

^eUsing the data of Ref. 34 and $\alpha = 2 - \beta(\delta + 1)$.

^fUsing the data of Ref. 34 and $\alpha = 2 - \gamma(\delta + 1)/(\delta - 1)$.

asymptotic region and $\alpha^* = 0$, $\epsilon = 0$ and $n = 3$ in the mean-field region. The value of A^+/A^- should thus be $1.36 \geq A^+/A^- \geq 0.75$ in the present material. Our results of $0.64 \geq A^+/A^- \geq 0.60$ show also that not all of the $|t|$ range is enclosed in the asymptotic region. It is not clear however why the experimentally obtained A^+/A^- is smaller than 0.75 but it is known that in the present material a small amount of imperfections can introduce anisotropy²² and, on the other hand, slight amounts of anisotropy can reduce the effective value of n .⁴² While there is no convincing evidence that this is indeed the case here, this possibility ($2 < n < 3$) might explain the A^+/A^- value as well as our α^* values and the exponents found in the magnetization measurements (see Table I). Whether this possibility is realized or not, a transition from mean-field to asymptotic behavior is clearly established here.

While it is widely held that reliable critical exponents can be obtained with data for which $t_{\max} \leq 10^{-3}$, in most Heisenberg ferromagnets^{14,15} the theoretically expected critical exponents and amplitude ratios were obtained in the region $10^{-1} > t > 10^{-4}$. The fact that this is not the case in the present material can be understood in view of the magnetic properties of the spinel B -site ferromagnets. It was shown that in these ferromagnets the weak interactions of the large number of next-nearest-neighbors B sites could even "outweigh the smaller number of stronger nearest-neighbor interactions."⁴³ The first are relatively long range considering the fact that they involve the fourth-nearest neighbors at a distance of $a(10)^{1/2}/4$, where a is the lattice constant, while the nearest neighbors are at a distance of $\frac{1}{4}a(2)^{1/2}$. On the other hand, it is well known that the Ginzburg-reduced temperature t_G is inversely proportional to $\xi_0^{2/\epsilon}$ where ξ_0 is in the range of the interaction.^{11,44} Hence, in the present case ($\epsilon = 1$), t_G may be smaller by a factor of 5 compared with t_G of a nearest-neighbor ferromagnet. The results of Eqs. (8) and (9) are also consistent with the knowledge⁴⁴ on t_G that enables an order of magnitude larger t_G for $T < T_c$, i.e., a smaller exponent for $T < T_c$ than for $T > T_c$, for a given $|t|$ interval.

In conclusion, we may say that the present optical data in the close vicinity of T_c are in accord with previous results on the magnetic energy-type dependence of the optical gap in ferromagnetic semiconductors. The temperature range studied, $10^{-1} \geq |t| \geq 5 \times 10^{-4}$, is found to be a transition region from mean-field behavior to asymptotic critical behavior. This behavior is understood in terms of the range of the magnetic interaction in the present material.

ACKNOWLEDGMENTS

The authors are thankful to H. Pinch for the crystals, to Mrs. L. Goldenberg for taking the magnetic moment measurements, and to S. Alexander for stimulating discussions.

APPENDIX A

Below T_c two contributions to the optical-gap shift are expected; one that has a magnetizationlike behavior and the other that has a magnetic energylike behavior. These originate from the second-order perturbation theory. In the mean-field region, both are expected to yield at $t^{1/2}$ dependence of the shift, and thus one can not distinguish between these contributions.

In the scaling region, the theory predicts that finally (with decreasing $|t|$) the $|t|^\beta$ term will dominate. The present experimental observations indicate that at least for $|t| \geq 5 \times 10^{-4}$ this is not the case. To get an estimate of the $|t| \equiv t_t$, for which a transition from a magnetic energylike to a magnetizationlike behavior is expected, let us examine the theoretical predictions.

Using Eq. (4.4) of Ref. 9, we find that the temperature-dependent part of ΔE for $T < T_c$, is

$$\Delta E = -\frac{1}{2}JS|t|^\beta + \frac{m^*J^2\Omega}{4(2\pi)^2\hbar^2k} \int_0^\Lambda dq q \left(\frac{q}{k} - \ln \left| \frac{q+2k}{q-2k} \right| \right) \Gamma_\alpha(|t|). \quad (\text{A1})$$

The integral can be separated into two regions: $2k > q \geq 0$ and $\Lambda \geq q > 2k$. Using the approximation

$$\ln \left| \frac{(q+2k)}{(q-2k)} \right| = 2 \left[\frac{q}{2k} + \frac{1}{3} \left(\frac{q}{2k} \right)^3 + \dots \right] \quad (\text{A2})$$

for $q < 2k$, and the dominant part of the correlation function, $\Gamma_\alpha = 2G_0 t^{-\nu} / x^{2-\eta+(1-\alpha)/\nu}$ (here $\alpha \equiv \alpha^*$) we get that the dominant term that has the $|t|^{1-\alpha}$ temperature dependence in the first region is

$$-\frac{1}{3} \int_0^{2k} dq q^4 \Gamma_\alpha = \frac{\frac{2}{3}G_0 k^{2-\eta+(1-\alpha)/\nu}}{[3+\eta-(1-\alpha)/\nu]}. \quad (\text{A3})$$

In the second region the corresponding dominant term is

$$\frac{1}{k} \int_{2k}^\Lambda dq q^2 \Gamma_\alpha = \frac{-2G_0 k^{2-\eta+(1-\alpha)/\nu} (2k)^{\eta-(1-\alpha)/\nu}}{1+\eta-(1-\alpha)/\nu}. \quad (\text{A4})$$

Using $\eta \approx 0$, $|\alpha| \leq \frac{1}{8}$, $\nu \approx \frac{2}{3}$ we obtain that the net contribution due to (A3) and (A4) is about

$$6G_0 k^{2-\eta+(1-\alpha)/\nu} (2k)^{\eta-(1-\alpha)/\nu}. \quad (\text{A5})$$

The only constant to be determined is G_0 . This can be done by using the sum rule and the correlation function defined by Eq. (2.10) of Ref. 9 in the limit $|t| \rightarrow 0$. This procedure [as can be

seen from Eq. (A6) in Ref. 9] yields

$$G_0 \kappa_0^{2-\eta} \Lambda^{1+\eta} = S(S+1)2\pi^2/\Omega. \quad (\text{A6})$$

By substituting Eqs. (A6) and (A5) in (A1) we get

$$\Delta E = (-\frac{1}{2}JS)\{|t|^\beta + [J(S+1)/4E_k] \\ \times (\kappa_0/k)^{(1-\alpha)/\nu-1-\eta} |t|^{1-\alpha}\}. \quad (\text{A7})$$

It should be noted that this is the critical behavior of an Ising ferromagnet ($\alpha > 0$). In general we have

to replace $t^{1-\alpha}$ by U^- recalling that the units to be selected are $A^-/\alpha \approx 1$.

The estimate of t_t assuming $\kappa_0 \approx \Lambda$ and $\alpha \approx \eta \approx 0$, is

$$|t| \approx [J(S+1)/4E_k]^{-3/2} (\kappa_0/k)^{-3/4}. \quad (\text{A8})$$

For example⁸ with $J = 0.5$ eV, $E_k = 0.05$ eV (see Fig. 1), $S = \frac{3}{2}$ and $\kappa_0/k \approx 12$ we get $t_t \approx 10^{-2}$. If U^- is introduced instead of $|t|^{1-\alpha}$ the value of t_t will be even larger.

- ¹P. Wachter, *CRC Crit. Rev. Solid State Sci.* **3**, 189 (1972).
- ²B. Batlogg, E. Kaldis, A. Schlegel, and P. Wachter, *Phys. Rev. B* **12**, 3940 (1975).
- ³ CdCr_2S_4 has an apparent blue shift, but more careful studies have shown that this is not the case. See, for example, S. B. Berger and L. Ekstrom, *Phys. Rev. Lett.* **23**, 1499 (1969); and S. Wittekoek and P. F. Bongers, *IBM J. Res. Dev.* **14**, 312 (1970).
- ⁴E. Callen, *Phys. Rev. Lett.* **20**, 1045 (1968).
- ⁵T. Kambara and Y. Tanabe, *J. Phys. Soc. Jpn.* **28**, 628 (1970).
- ⁶M. J. Freiser, F. Holtzberg, S. Methfessel, G. D. Petit, M. W. Shafer, and J. C. Suitz, *Helv. Phys. Acta.* **41**, 832 (1968).
- ⁷F. Rys, J. S. Helman, and W. Baltensperger, *Phys. Kond. Materie* **6**, 105 (1967).
- ⁸C. Haas, *Phys. Rev.* **168**, 531 (1968).
- ⁹S. Alexander, J. S. Helman, and I. Balberg, *Phys. Rev. B* **13**, 304 (1976).
- ¹⁰J. S. Helman, I. Balberg, and S. Alexander, *AIP Conf. Proc.* **21**, 495 (1976).
- ¹¹L. P. Kadanoff, W. Götze, D. Hamblen, R. Hecht, E. A. S. Lewis, V. V. Palciausaka, M. Rayl, J. Swift, D. Aspens, and J. Kane, *Rev. Mod. Phys.* **39**, 395 (1967).
- ¹²E. Brézin, J. C. Le Guillou, and J. Zinn-Justin, *Phys. Lett. A* **47**, 285 (1974); *Phys. Rev. B* **8**, 5330 (1973); and *Phase Transitions and Critical Phenomena*, edited by C. Domb and M. S. Green (Academic, New York, to be published), Vol. VI.
- ¹³B. J. C. van der Hoeven, Jr., Dale T. Teaney, and V. L. Moruzzi, *Phys. Rev. Lett.* **20**, 719 (1968).
- ¹⁴F. L. Lederman, M. B. Salamon, and L. W. Schacklette, *Phys. Rev. B* **9**, 2981 (1974).
- ¹⁵A. Kornblit and G. Ahlers, *Phys. Rev. B* **11**, 2678 (1975).
- ¹⁶J. C. Suits, *J. Appl. Phys.* **38**, 1498 (1967).
- ¹⁷A. Brooks Harris, *J. Phys. C* **17**, 1671 (1974).
- ¹⁸G. Harbeke and H. Pinch, *Phys. Rev. Lett.* **17**, 1090 (1966).
- ¹⁹H. L. Pinch and L. Ekstrom, *RCA Rev.* **31**, 692 (1970).
- ²⁰H. L. Pinch and S. B. Berger, *J. Phys. Chem. Solids* **29**, 2091 (1968); and P. J. Wojtowicz, S. B. Berger, and H. L. Pinch, *RCA Report No. AFCRL-70-00-45*, RCA Laboratories, Princeton N.J. (1970) (unpublished). (Available from NTIS Springfield, Va. 22151.)
- ²¹A. Amith and L. Friedman, *Phys. Rev. B* **2**, 434 (1970); and A. Amith, S. B. Berger, and P. J. Wojtowicz, *RCA Report No. AFCRL-71-00-29*, RCA Laboratories, Princeton, N.J. (1971) (unpublished). (Available from NTIS Springfield, Va. 22151.)
- ²²P. K. Baltzer, M. Robbins, and P. J. Wojtowicz, *J. Appl. Phys.* **38**, 953 (1967); and *J. Phys. Chem. Solids* **28**, 2423 (1967).
- ²³R. A. Craven and R. D. Parks, *Phys. Rev. Lett.* **31**, 383 (1973).
- ²⁴I. Balberg, A. Maman, and A. Margalit, in *Proceedings of the Thirteenth International Conference on the Physics of Semiconductors*, edited by F. Fumi (Marves, Rome, to be published).
- ²⁵T. Itoh, N. Miyata, and S. Nayita, *Jpn. J. Appl. Phys.* **12**, 1265 (1973).
- ²⁶K. Miyatani, F. Okamoto, P. K. Baltzer, S. Osaka, and T. Oka, *AIP Conf. Proc.* **17**, 285 (1972).
- ²⁷H. Fujita, Y. Okada, and F. Okamoto, *J. Phys. Soc. Jpn.* **31**, 610 (1971).
- ²⁸J. Schoenes and P. Wachter, *Phys. Rev. B* **9**, 3097 (1974).
- ²⁹We found, for example, that $\text{Cd}_{1-x}\text{In}_x\text{Cr}_2\text{Se}_4$ crystals with $x = 0.014$ have a total red shift that is by a factor of $\frac{2}{3}$ smaller than the shift shown in Fig. 2(a).
- ³⁰F. C. Zumsteg and R. D. Parks, *Phys. Rev. Lett.* **24**, 520 (1970).
- ³¹D. W. Marquardt, *J. Soc. Indust. Appl. Math.* **11**, 43 (1963); and Share (IBM) General program Library DPE NLIN (LS) 3094 (unpublished, 1964).
- ³²A. Kornblit and G. Ahlers, *Phys. Rev. B* **8**, 5163 (1973).
- ³³B. Golding, *Phys. Rev. Lett.* **27**, 1142 (1971).
- ³⁴K. Miyatani, *J. Phys. Soc. Jpn.* **28**, 259 (1970).
- ³⁵D. S. Simons and M. B. Salamon, *Phys. Rev. B* **10**, 4680 (1974).
- ³⁶F. Holtzberg, T. R. McGuire, T. Penney, M. W. Shafer, and S. Van Molnar, *IBM Final Technical Report*, ARPA Order No. 1588, June 1971 (unpublished).
- ³⁷G. W. Martin, A. T. Kellogg, R. L. White, R. M. White, and H. Pinch, *J. Appl. Phys.* **40**, 1015 (1969).
- ³⁸H-h. Chou and H. Y. Fan, *Phys. Rev. B* **10**, 901 (1974).
- ³⁹M. Taniguchi, Y. Kato, and S. Narita, *Solid State Commun.* **16**, 261 (1975).
- ⁴⁰M. Ferer, M. A. Moore, and M. Wortis, *Phys. Rev. B* **1**, 3954 (1971); **8**, 5205 (1973).
- ⁴¹D. J. Wallace, in *Phase Transitions and Critical Phenomena*, edited by C. Domb and M. S. Green (Academic, New York, to be published).
- ⁴²H. E. Stanley, *Introduction to Phase Transitions and Critical Phenomena* (Clarendon, Oxford, 1971).
- ⁴³P. K. Baltzer, P. J. Wojtowicz, M. Robbins, and E. Lopatin, *Phys. Rev.* **151**, 367 (1966).
- ⁴⁴D. J. Amit, *J. Phys. C* **7**, 3369 (1974).